

Synchronization of non-chaotic dynamical systems

F. Bagnoli*

Dipartimento di Matematica Applicata, Università di Firenze, Via S. Marta, 3 I-50139 Firenze

F. Cecconi**

International School for Advanced Studies (SISSA/ISAS) via Beirut 2-4, I-34014 Trieste

(February 5, 2020)

Abstract

A synchronization mechanism driven by annealed noise is studied for two replicas of a coupled-map lattice which exhibits *stable chaos* (SC), i.e. irregular behavior despite a negative Lyapunov spectrum. We show that the observed synchronization transition on changing the strength of noise belongs to the directed percolation universality class. This result is consistent with the behavior of *chaotic* deterministic cellular automata (DCA), supporting the equivalence Ansatz between SC and DCA. The noise threshold after which two replicas of the system synchronize is strictly related to the propagation velocity of perturbations in the system.

I. INTRODUCTION

The occurrence of disordered patterns and their propagation in the presence of a negative Lyapunov spectrum have been often observed in spatiotemporal systems [1–5]. One can classify this kind of irregular behavior into two general groups with basically different features: *transient chaos* and *stable chaos*.

Transient chaos (TC) is a truly chaotic regime with finite life time, characterized by the coexistence in the phase space of stable attractors and chaotic non attracting sets named chaotic saddles or repellers [6]. Starting from a generic configuration, the system typically exhibits irregular transient behavior before collapsing abruptly onto a nonchaotic attractor. Lyapunov exponents, being defined as asymptotic quantities, are not able to detect the presence of transiently chaotic states. The repelling features of saddles are numerically revealed by computing the finite-time (or effective) maximum Lyapunov exponent, and averaging over the ensemble of trajectories which have not yet left a certain neighborhood of the repeller at a given time [7]. One thus observes that this quantity fluctuates around a positive value during the transient [5] and switches to negative values after the transition to the stable attractor.

Stable chaos (SC) constitutes a different kind of irregular behavior [1,2], where the transient evolution appears highly complex even though all finite-time Lyapunov exponents become rapidly negative. Moreover, in SC systems, lifetimes of transient regimes may scale exponentially with the system size (supertransients [1,2]) so that the final stable attractor is practically never reached for large enough systems. One is thus allowed to assume that such regime may be of substantial experimental interest and becomes the only physically relevant state in the thermodynamic limit.

While TC is clearly associated to information production, i.e. to the response of the system to infinitesimal disturbances, SC is mainly related to propagation and mixing of information. In other words SC systems are sensitive only to *finite* perturbations [8], reacting like stable systems to infinitesimal ones, as we discuss in Section II through an example.

Although SC behavior has been observed in several models such as coupled map lattices [1–3] and oscillators [4], no clear explanation of its origin still exists.

As already pointed out in Ref. [2], SC-behavior is very reminiscent of the phenomenology of deterministic cellular automata (DCA). Indeed, in finite size DCA, only limit cycles and fixed points are allowed as attractors, since the state variables assume discrete values and thus the number of possible configurations is finite. Nevertheless, transient regimes may appear very irregular and the corresponding lifetimes may grow exponentially with the system size. According to Wolfram classification [9], these DCA's constitute the third (“chaotic”) class. The emergence of such a complex behavior is clearly illustrated by the damage spreading analysis [10,11], in which two replicas of the model evolve starting by slightly different initial conditions. An initial difference spreads through the whole system in chaotic DCA, while it eventually freezes or disappears in nonchaotic ones. A similar scenario has been observed in continuous systems exhibiting SC [3]. Although a general symbolic mapping of SC- onto DCA-models is not yet available, the statement that chaotic DCA represent a subclass of SC systems is reasonable: what is known about DCA can be automatically translated into the language of SC. It is worth stressing that the advantage of SC over DCA is the existence of continuous control parameters.

Although the standard Lyapunov analysis is not able to characterize the irregular features of SC behavior, it can be complemented by the study of a suitable synchronization mechanism, already used in Ref. [12] to classify the chaotic properties of DCA. The basic idea consists of measuring the amount of “pinching” required to synchronize a replica (slave) to the original system (master). The master-slave interaction is a stochastic, spatially extended version of the Pecora-Carroll synchronization mechanism [13]. Each time step is composed by two phases: in the first one the master and slave system evolve freely according with the same evolution equation, and then a fraction p of the degrees of freedom of the slave system is set to the same value of the corresponding degrees of freedom of the master one. Synchronization of spatially extended systems has been usually studied with symmetrical interactions [14–17]. Our asymmetric scheme, instead, allows probing the dynamical properties of the master system. By increasing p from 0, the dynamics of slave system tends to synchronize to that of master, and the pinching synchronization transition (PST) occurs. The threshold p -value, above which the two replicas synchronize, is a suitable indicator of the chaotic spatial behavior of the unperturbed system (master). In DCA the pinching synchronization transition belongs to the directed percolation (DP) universality class [12,17], while in chaotic continuous systems (e.g. coupled map lattices) the synchronization is never perfect for finite times, nor it is equivalent to an absorbing state [17]. This might imply non-DP scaling exponents [18–20].

In this paper, we first illustrate the key differences between SC and TC through a clarifying toy model (Section II). Then in Section III, following the close analogy between SC and DCA, we study the PST for a model considered in Ref. [3]. We find that even for that model the PST is well defined, and our numerical results support the hypothesis that such a transition belongs to the DP universality class. Moreover, we show that the PST phase diagram is consistent with that reported in Ref. [3] for the damage spreading velocities.

II. TRANSIENT AND STABLE CHAOS

In this section we introduce and discuss a spatiotemporal model in which the main differences between SC and TC are easily illustrated.

Let us consider the one-dimensional coupled-map lattice (CML), i.e. an array of state variables $\{x_1, \dots, x_L\}$ in the interval $[0, 1]$ subject to the discrete-time evolution rule

$$x_i(t+1) = g(x_{i-1}(t), x_i(t), x_{i+1}(t)). \quad (1)$$

Each site-variable x_i interacts diffusively with its nearest neighbors

$$g(u, v, z) = (1 - 2\varepsilon)f(u) + \varepsilon[f(u) + f(z)]. \quad (2)$$

We always used $\varepsilon = 1/3$. The local mapping has the form showed in Fig. 1:

$$f(x) = \begin{cases} 0 & \text{for } 0 \leq x < \alpha, \\ \frac{x - \alpha}{1/3 - 2\alpha} & \text{for } \alpha \leq x < 1/3 - \alpha, \\ 1 & \text{for } 1/3 - \alpha \leq x < 1/3 + \alpha, \\ 1 - \frac{x - 1/3 - \alpha}{1/3 - 2\alpha} & \text{for } 1/3 + \alpha \leq x < 2/3 - \alpha, \\ 0 & \text{for } 2/3 - \alpha \leq x < 2/3 + \alpha, \\ \frac{x - 2/3 - \alpha}{1/3 - 2\alpha} & \text{for } 2/3 + \alpha \leq x < 1 - \alpha, \\ 1 & \text{for } 1 - \alpha \leq x < 1. \end{cases} \quad (3)$$

First, we discuss the case of infinite slope map, (i.e. $\alpha = 1/6$, full line in Fig. 1) corresponding to SC regime. In fact, after one time step, each configuration of the lattice reduces to a sequence of “0” and “1” (Boolean configuration). The system evolution remains, however, irregular since, for this value of α , this model is equivalent to a deterministic cellular automaton (DCA) with the *rule 150*, which is known to generate highly irregular patterns [9]. On the other hand, to explain such an irregular behaviour one cannot invoke either chaotic saddles or local fluctuations of the Lyapunov exponent, the latter being always $-\infty$, due to the particular form of the map. Although this system is totally insensitive to infinitesimal perturbations, finite perturbations of amplitude greater than $1/6$ gives rise to a “defect” which evolves following the *rule 150* as well (the rule 150 is additive modulo two) and propagates through the lattice.

A slight tilting of the vertical edges of the map, ($0 < \alpha < 1/6$, dotted and dashed lines in Fig. 1) introduces some expanding regions in the phase space. Accordingly, one obtains a typical TC behaviour, resulting here from the competition between stable and unstable effects, followed by a SC regime.

The TC properties of system trajectories are shown by studing the tangent dynamics and finite-time Lyapunov exponent

$$\gamma(t) = \frac{1}{t} \log \frac{|\mathbf{z}(t)|}{|\mathbf{z}(0)|},$$

where \mathbf{z} indicates a generic tangent vector which evolves following the linearization of the dynamics of Eqs. (1–3). A typical time fluctuation of the local expansion rate $\mu(t) = |\mathbf{z}(t)|/|\mathbf{z}(t-1)|$ (or local multiplier) is shown in Fig. 3 for $\alpha = 0.052$. The irregularity of the signal is an indication of chaotic-like behavior of the system. The simulation is stopped at time T_r when $\mathbf{z}(t)$ becomes exactly $\mathbf{0}$, i.e. when the system settles down into a SC configuration (Boolean state) which is Lyapunov-stable by definition. In this sense T_r provides an estimate for the transient-chaos lifetime.

For trajectories which have not yet entered binary configurations at time t , $\gamma(t)$ remains positive, as seen in Fig. 4, where the distribution of $\gamma(t)$ is shown for a set of 2000 trajectories starting from arbitrary initial conditions.

The lifetime T_r of the TC regimes preceding the SC behavior depends on α , and becomes shorter as α approaches $1/6$, value at which the system behaves as a true DCA after just

one time step. In the limit $\alpha \rightarrow 0$, the flat regions of the map disappear (the slope being equal to 3) and TC regimes become persistent so that they degenerate into fully developed chaos (FDC).

A more detailed analysis of the behavior of the model of Eqs. (1–3) upon changing the control parameter α will be presented elsewhere. Here such a qualitative discussion has the only aim to highlight the key differences between SC and TC dynamics, both present in this toy model.

The observed SC regime occurs only as a DCA behavior. In fact, as soon as the system falls into a Boolean configuration, it evolves as a genuine chaotic DCA. In the following section we discuss a more general SC model whose behavior does not trivially reduce to chaotic DCA, in particular we study the synchronization properties of two replicas of that system.

III. THE MODEL AND THE SYNCHRONIZATION DYNAMICS

The dynamical system considered is the one-dimensional CML of Eqs. (1,2) with the coupling constant $\varepsilon \in [0, 1/2]$ and periodic boundary conditions over a length L (system size). The local mapping has the form

$$f(x) = \begin{cases} bx & \text{if } 0 < x < 1/b \\ a + c(x - 1/b) & \text{if } 1/b < x < 1 \end{cases} \quad (4)$$

We use here the parameter values $\{a = 0.07, b = 2.70, c = 0.10\}$ of Ref. [3] for which the map of Eq. (4) is attracted into a stable period-3 orbit. An example of the space-time evolution of the CML is shown in Fig. 5. In the previous section, the analyzed SC behavior was actually equivalent to a DCA dynamics, in this case the model never relaxes into a real cellular automaton state.

In Ref. [3] an ε -dependent dynamical phase transition between periodic and chaotic regimes of this system has been carefully investigated by damage spreading analysis. The ordered (chaotic) phase is characterized by the absence (presence) of damage propagation. Therefore, the damage spreading velocity can be considered a good indicator for this transition. It turns out from Ref. [3], that for $\varepsilon < \varepsilon_c^{(1)} \simeq 0.3$ only periodic phases are observed, for $\varepsilon > \varepsilon_c^{(2)} \simeq 0.3005$ only chaotic states exist, while in the intermediate region $\varepsilon \in [\varepsilon_c^{(1)}, \varepsilon_c^{(2)}]$, periodic and chaotic behaviors alternate in an apparently irregular manner (fuzzy region).

We study the effects of the pinching synchronization on this model, and its interplay with the above described transition.

The master system follows the dynamics described in Eq. (1), while the slave system evolves as

$$y_i(t+1) = [1 - r_i(t)]g(y_{i-1}(t), y_i(t), y_{i+1}(t)) + r_i(t)g(x_{i-1}(t), x_i(t), x_{i+1}(t)) \quad (5)$$

where $r_i(t)$ is a Boolean random variable

$$r_i(t) = \begin{cases} 1 & \text{with probability } p, \\ 0 & \text{otherwise.} \end{cases}$$

Practically, at each time step, a fraction p of site variables in the slave system are set equal to the corresponding variables of the master (see. Fig. 6).

The synchronization order-parameter is the asymptotic value of the topological distance ρ between master and slave systems (i.e. the fraction of non synchronized sites)

$$\rho(t, p) = \lim_{L \rightarrow \infty} \frac{1}{L} \sum_{i=1}^L \Theta(|x_i(t) - y_i(t)|) \quad (6)$$

where $\Theta(s)$ is the unitary step-function. We denote by p^* the synchronization threshold, such that $\rho(\infty, p < p^*) > 0$ and $\rho(\infty, p < p^*) = 0$. This synchronization mechanism defines an associated directed site-percolation problem in $d = 1 + 1$ dimension, where a site of coordinate (i, t) is “wet” if $r_i(t) = 0$ and it is connected to at least one neighboring wet site at time $t - 1$. At $t = 0$ all sites are assumed to be wet. We denote by p_c the critical threshold for which a cluster of wet sites percolates along the time direction. The master and the slave systems can stay different only on the cluster of wet sites.

For chaotic CMLs two synchronization scenarios are possible, called *weak* and *strong* chaos respectively [21]. A system is said strongly chaotic if it does not synchronize even on the critical wet cluster (i.e. for $p^* = p_c$) and therefore the distance ρ of Eq. (6) always exhibits DP scaling. Alternatively one can say that for strongly chaotic systems, the active and the wet clusters are essentially the same for every value of p .

Instead, for weakly chaotic systems, the synchronization threshold p^* is always located below p_c and the transition is discontinuous (first-order like). For $p < p^*$ again the active and wet clusters coincide, whereas for $p > p^*$ the active cluster disappears, but the wet cluster still percolates. Such a behavior is due to the exponential vanishing of the difference field $\mathbf{h}(t) = \{x_i(t) - y_i(t)\}_{i=1}^L$, even though local fluctuations of \mathbf{h} can sporadically appear.

Conversely, DCAs [12] always synchronize at p^* below p_c (i.e. synchronization occurs in presence of the percolating wet cluster) but $\rho(t, p)$ still exhibits DP scaling. This is a straightforward consequence of the finiteness of the number of states in DCAs, which prevents fluctuations of \mathbf{h} in the absorbing state. We show in the following that the latter scenario holds also for SC systems.

IV. NUMERICAL RESULTS

A first set of simulations has been performed for lattices of size $L = 3000$, with periodic boundary conditions. We measured $\rho(t, p)$ at different times and the results have been averaged over a 5000 randomly chosen initial conditions. For each simulation a transient of 10^4 time steps has been discarded in order to avoid initial bias and reach stationary states. A site i is considered to be synchronized (and $y_i(t + 1)$ is set equal to $x_i(t + 1)$) if $|y_i(t) - x_i(t)| < \tau$, where τ is a sensibility threshold. In this way we can control the effects of the finite precision of computer numbers. We checked that the results are independent of τ (for small τ), and we choose $\tau = 10^{-8}$ for massive simulations.

A typical behavior of $\rho(t, p)$ near p^* is shown in Fig. 7. The value of p corresponding to the most straight curve at large t represents the best approximation of p^* , which can be estimated with good accuracy (black dots of Fig. 9). The straight dashed line indicates the DP scaling results.

For those values of ε for which the above analysis provided a too uncertain result in the estimation of p^* , we have carried out single-site simulations for larger systems, obtaining a more accurate determination of p^* . These simulations consist in preparing the slave system exactly synchronized to the master except for the central site, and in measuring how non-synchronized sites propagate throughout the system, generating DP-like clusters. This method probes the stability of synchronized states with respect to minimal perturbations.

As usual in this type of simulations, we measured the survival probability $P(t)$ of the desynchronized states, the number of non synchronized sites $N(t)$, and their second moment $R^2(t)$ with respect to the center of the lattice (generally called the gyration radius). Near the synchronization threshold and in the long time limit, these magnitudes are expected to scale as [22,23]

$$N(t) \sim t^\eta, \quad P(t) \sim t^{-\delta}, \quad R^2(t) \sim t^z. \quad (7)$$

The determination of the asymptotic value of such exponents (e.g. η) is performed by plotting the effective exponent

$$\bar{\eta}(t) = \frac{\log(N(at))}{\log(N(t))}$$

versus $1/t$ for several values of p . Here a denotes an arbitrary scale factor (here we always used $a = 2$). In the limit $t \rightarrow \infty$ $\bar{\eta}$ converges to η for $p = p^*$, and diverges for other values of p . In pure DP systems this method allows the simulation of effectively infinite lattices, since the reference state, i.e. the absorbing one (usually made of "0"s) is unique and does not change in time. Conversely, in our case the absorbing state coincides with the synchronized state and this implies the detailed knowledge of the evolution of the master system. This circumstance imposes severe limitations on lattice sizes and performances of the method.

In Figure 8 we report the behavior of the effective exponents $\bar{\eta}$, $\bar{\delta}$ and $\bar{z} + \bar{\eta}$ versus $1/t$ for several values of p . The asymptotic values of the exponents ($\eta = 0.330(5)$, $\delta = 0.13(2)$, $z = 1.25(2)$) are consistent with the best known DP ones ($\eta = 0.31368(4)$, $\delta = 0.15947(3)$, $z = 1.26523(3)$ [23]).

This analysis, repeated for several values of ε , indicates that the synchronization of SC systems reasonably belongs to the DP universality class. The very slow convergence of the system dynamics to the asymptotic state makes hard to exclude that for some values of ε the DP character of the transition is violated. However, we believe that, owing to the stability of the model of Eqs. (1,2,3), small local disturbances are re-absorbed at exponential rate, and cannot generate desynchronization effects. In other words, the synchronized state is absorbing with respect to small fluctuations. This is also consistent with the fact that the simulation results are independent of the precision threshold τ . Therefore the local stability guarantees that for what concerns synchronization properties, SC systems behave mainly like discrete ones and differently from continuous chaotic systems. This is further support to the "*equivalence Ansatz*" between SC and DCA.

Indeed, preliminary simulations show that the DP scenario holds even if the local pinching is performed only up to a small difference Δ . This remark suggests the possibility of defining a finite-size maximum Lyapunov exponent, in a way similar to Ref. [24]. Further work in this direction is in progress.

Finally, the PST phase diagram is shown in Fig. 9, where p^* is plotted versus ε . The behavior of p^* is compared with that of the damage spreading velocity V_F (Ref [3]), properly re-scaled. These two phase diagrams are consistent, including the fuzzy region suggesting that both indicators (synchronization threshold and damage spreading velocity) characterize different aspects of the same phenomenon.

V. CONCLUSIONS

In summary, we have applied the pinching synchronization method to systems showing stable chaos. As in the cellular automata case, we have found that even in this continuous case the pinching synchronization transition (PST) is well defined, and that this transition belongs to the DP universality class. Our results shows that the stable chaos is indeed equivalent to cellular automata “chaoticity” and definitively different from transient chaos. The PST phase diagram is consistent with that reported in Ref. [3] for damage spreading velocities, including the fuzzy region.

ACKNOWLEDGMENTS

We thank A. Politi and R. Livi for useful discussions. We also thank all the components of the D.O.C.S. research group of Firenze (<http://docs.de.unifi.it/~docs>) for stimulating discussions and interactions.

REFERENCES

- * Also INFM Unità di Ricerca di Firenze and INFN Sezione di Firenze, L.go E. Fermi 2, 50125 Firenze, Italy; electronic address: bagnoli@dma.unifi.it
- ** Also INFM Unità di Ricerca di Trieste (Sissa); electronic address: cecconi@sissa.it
- [1] J.P. Crutchfield and K. Kaneko, Phys. Rev. Lett. **60**, 2715 (1988), K. Kaneko, Phys. Lett. **149A**, 105 (1990).
- [2] A. Politi, R. Livi, G.-L. Oppo, and R. Kapral, Europhys. Lett. **22**, 571 (1993).
- [3] F. Cecconi, R. Livi and A. Politi, Phys. Rev. E **57**, 2703 (1998).
- [4] R. Bonaccini and A. Politi, Physica D **103**, 362 (1997).
- [5] Y-C Lai and R.L. Winslow, Phys. Rev. Lett. **74**, 5208 (1995).
- [6] T. Tel, *Proceedings of the 19th IUPAP International Conference on Statistical Physics*, edited by Hao Bai-lin (World Scientific Publishing: Singapore 1996)
Directions in Chaos, vol.3, edited by Hao Bai-lin (World Scientific Publishing: Singapore 1990)
- [7] E. Ott, *Chaos in dynamical systems* (Cambridge University Press: Cambridge UK 1993).
- [8] A. Politi and A. Torcini, Europhys. Lett. **28**, 545 (1994).
- [9] S. Wolfram, Rev. Mod. Phys. **55**, 601 (1983).
 S. Wolfram (editor), *Theory and Application of Cellular Automata* (World Scientific, Singapore, 1986).
- [10] P. Grassberger, J. Stat. Phys. **79**, 13 (1995).
- [11] F. Bagnoli, J. Stat. Phys. **79**, 151 (1996).
- [12] F. Bagnoli and R. Rechtman, Phys. Rev. E **59**, R1307 (1999).
- [13] L.M. Pecora and T.L. Carroll, Phys. Rev. Lett. **64**, 821 (1990).
- [14] A. Maritan and J.R. Banavar, Phys. Rev. Lett. **72**, 1451 (1994).
- [15] D.H. Zanette and A.S. Mikhailov, Phys Rev. E **58**, 872 (1998).
- [16] F.S. de San Roman, S. Boccaletti, D. Masa and H. Mancini, Phys. Rev. Lett. **81**, 3639 (1998).
- [17] P. Grassberger, Phys. Rev. E **59**, R2520 (1999).
- [18] P. Grassberger, in *Proceedings of 1995 Shimla Conference on Complex Systems*, edited by S. Puri *et al.* (Narosa Publishing, New Delhi, 1997).
- [19] A.S. Pikovsky and J. Kurths, Phys. Rev. E **49**, 898 (1994).
- [20] G. Grinstein, M.A. Muñoz and Y. Tu, Phys. Rev. Lett. **76**, 4376 (1996).
- [21] F. Bagnoli, L. Baroni, and P. Palmerini, Phys Rev. E **59**, 409 (1999).
- [22] P. Grassberger and A. de la Torre, Ann. Phys. (N.Y.) **122**, 373 (1979).
- [23] M.A. Mugnoz, R. Dickman, A. Vespignani and S. Zapperi, cond-mat/9811287.
- [24] F. Bagnoli, R. Rechtman and S. Ruffo, Phys. Lett. A **172**, 34 (1992).

FIGURES

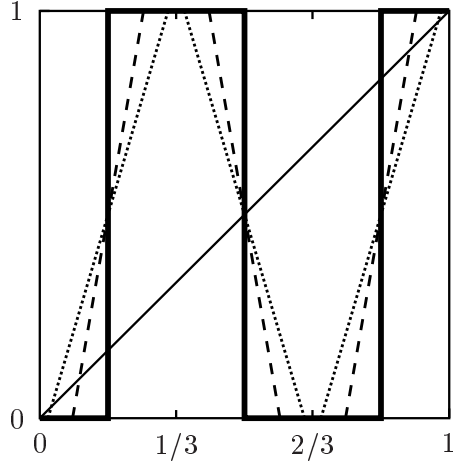


FIG. 1. Plot of the map of Eq. (3) for different values of α : $\alpha = 0.02$ (dotted line), $\alpha = 0.08$ (dashed line) and $\alpha = 1/6$ (continuous line).

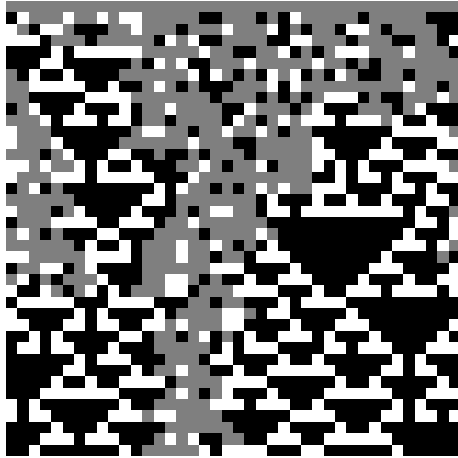


FIG. 2. Grayscale representation of space-time evolution of model of Eq. (2) with $\varepsilon = 1/3$ and $\alpha = 0.068$. Time runs from top to bottom, white (black) color indicates $x_i(t) = 0$ ($x_i(t) = 1$), while gray indicates all other values.

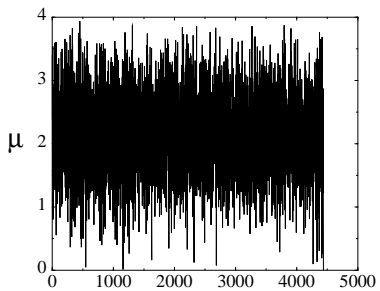


FIG. 3. Time behaviour of Lyapunov multiplier $\mu(t) = |\mathbf{z}(t)|/|\mathbf{z}(t-1)|$ for CML of Eq. (2) with $\alpha = 0.052$. The simulation is stopped at time $T_r = 4455$ when the system reaches the absorbing SC state.

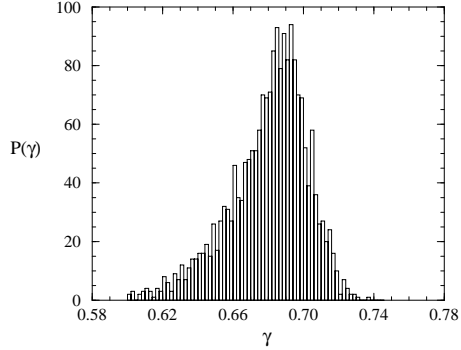


FIG. 4. Histogram of the finite-time Lyapunov exponent γ of model of Eq. (2) computed from a set of 2000 arbitrary initial conditions, with $\alpha = 0.052$. The size of the system is $L = 3000$ sites. For each initial condition, the evolution of Eq. (2) and its linearization are iterated until the system approaches a Boolean configuration.

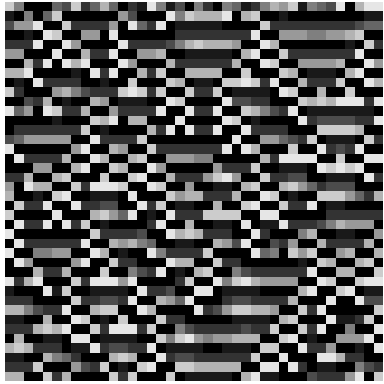


FIG. 5. Space-time evolution of the map Eq. 4, with $\varepsilon = 0.32$. Grayscale from $x_i(t) = 0$ (white) to $x_i(t) = 1$ (black).

MASTER

X_i

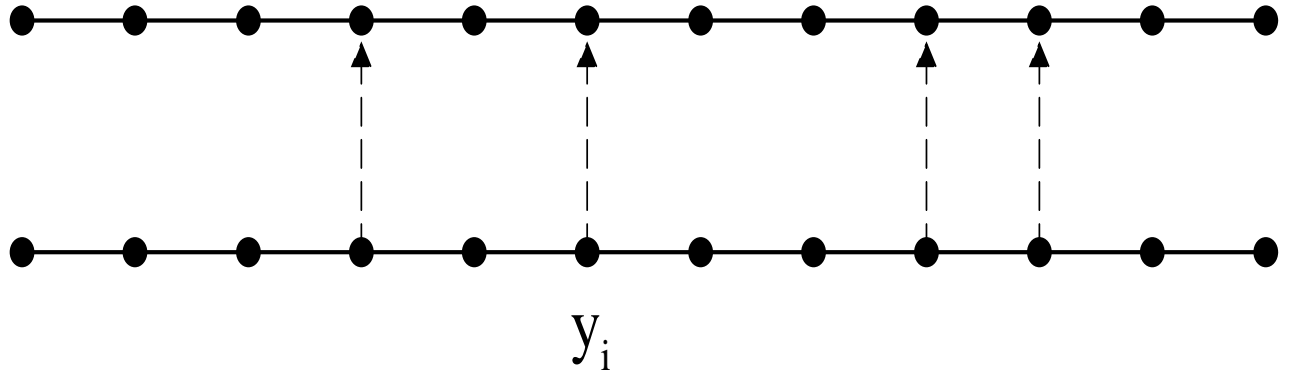


FIG. 6. Schematic representation of the pinching synchronization. Vertical dashed lines indicate the sites of the slave system identified to those of the master corresponding to $r_i = 1$ in Eq. (5).

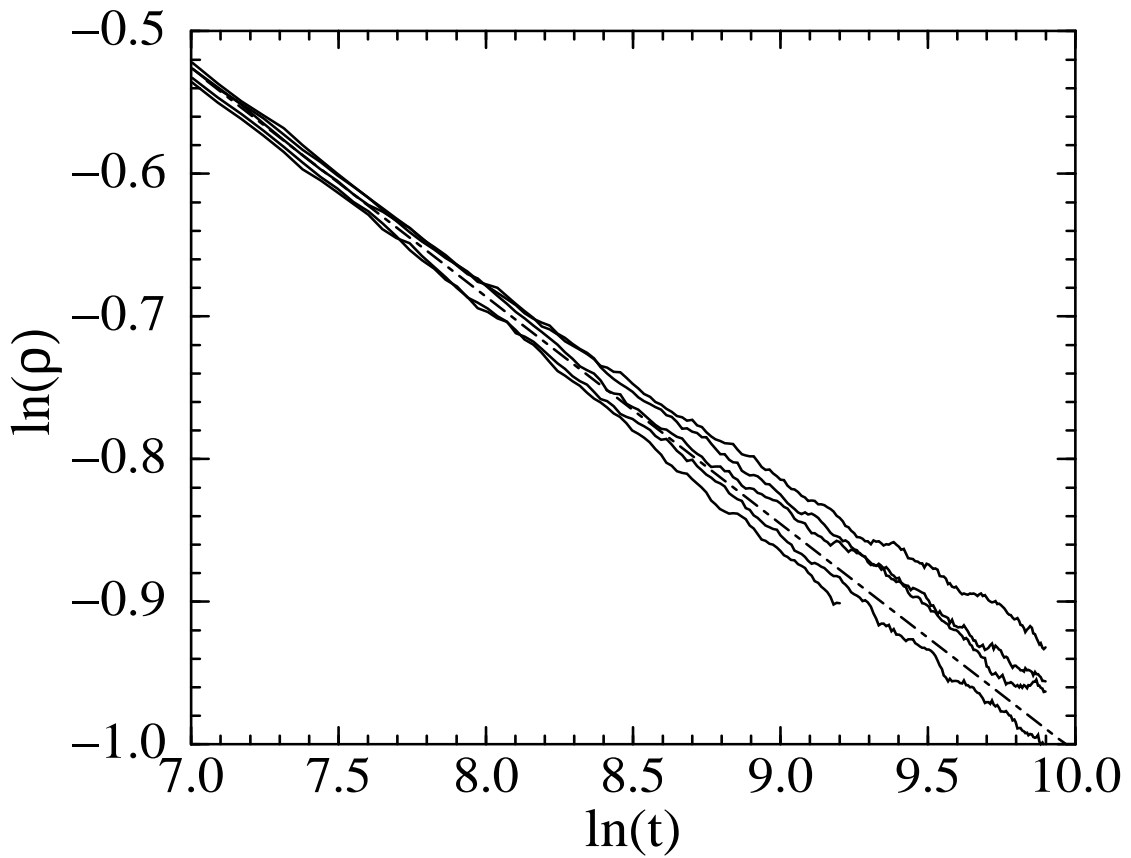
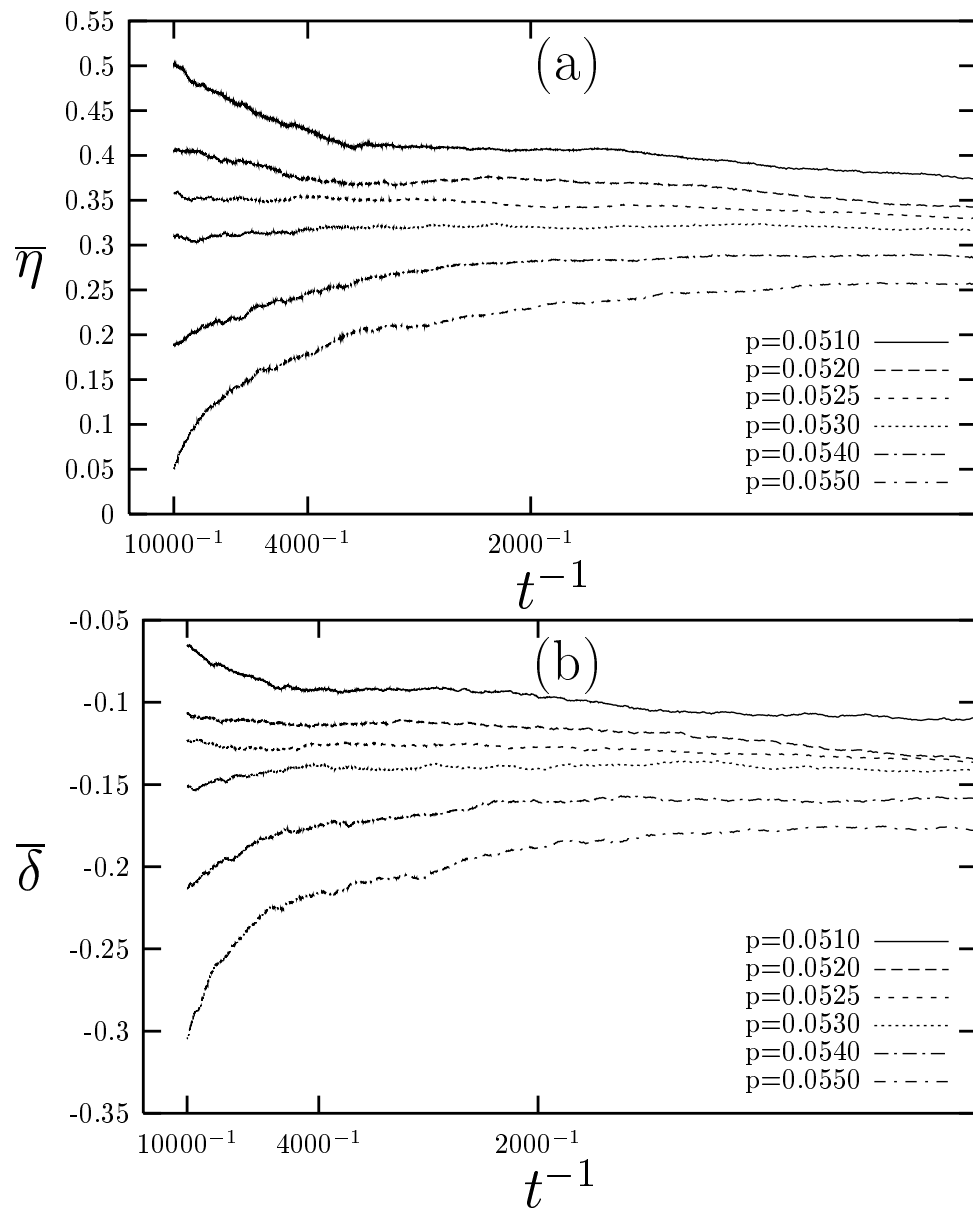


FIG. 7. Log-log plot of the order parameter $\rho(t, p)$ vs. t , for $p = 0.1269, 0.1270, 0.1271\dots$ from top to down, and for $\varepsilon = 0.305$. The dot-dashed straight line indicates the critical DP scaling $t^{-\delta}$ with $\delta = 0.159$. The estimated synchronization threshold turns to be $p^* = 0.1272(1)$.



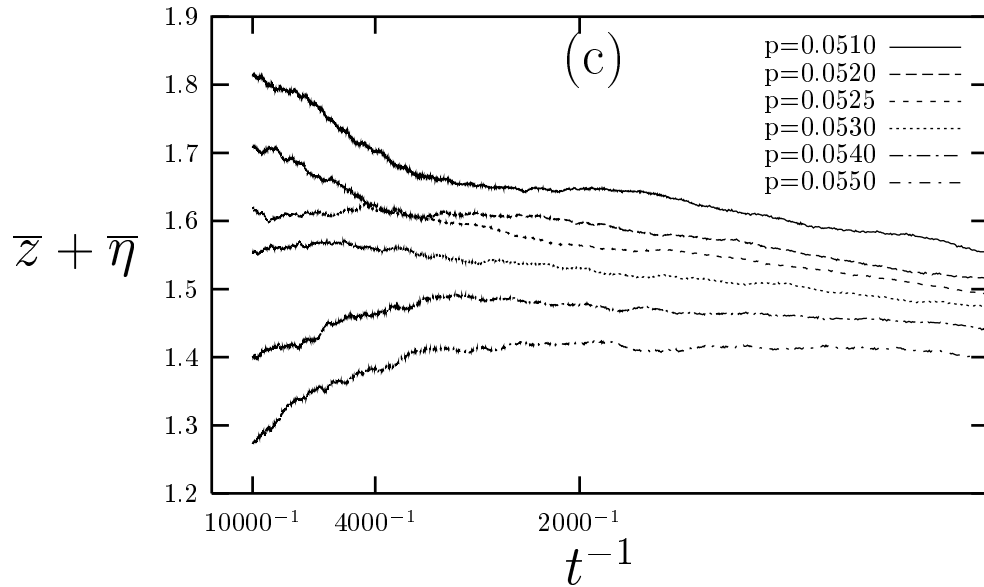


FIG. 8. effective exponents $\bar{\eta}(t)$ (a), $\bar{\delta}(t)$ (b) and $\bar{z}(t) + \bar{\eta}(t)$ (c) for $\varepsilon = 0.3004$ and several values of p . The average is taken over 50.000 runs, $a = 2$ and $L = 2000$.

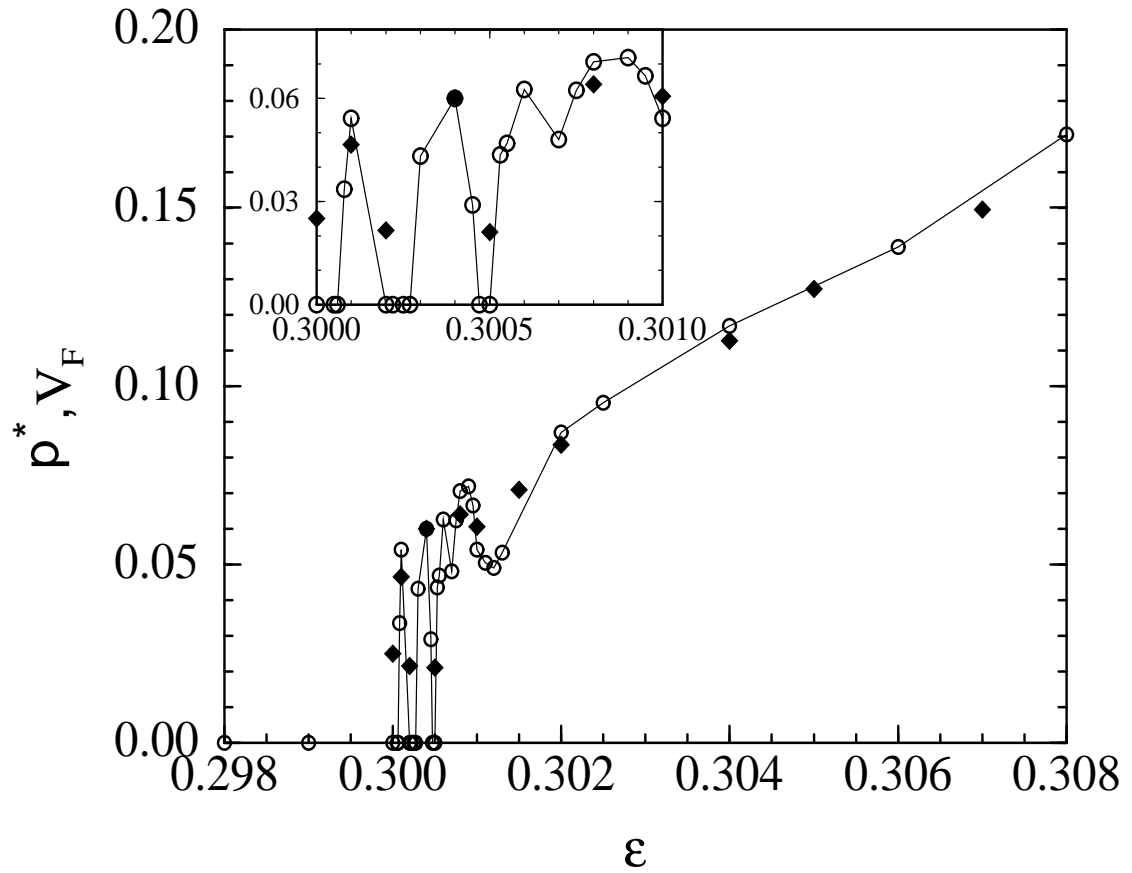


FIG. 9. Dependence of the synchronization threshold p^* on the coupling constant ε (diamonds) compared with the behaviour of V_F (open circles), the V_F -values are properly re-scaled. In the inset an enlargement of the region around $\varepsilon = 0.3$ is shown. The line is a guide to eye.